Mode Control and Pattern Stabilization in Broad-Area Lasers by Optical Feedback

J. Martín-Regalado †, G.H.M. van Tartwijk†*, S. Balle†‡, and M. San Miguel†‡
†Departament de Física, Universitat de les Illes Balears (UIB)
E-07071 Palma de Mallorca, Spain
‡Instituto Mediterraneo de Estudios Avanzados IMEDEA (CSIC-UIB)
E-07071 Palma de Mallorca, Spain
*Current address: The Institute of Optics, University of Rochester, Rochester, NY 14627.

Broad-area lasers exhibit complex spatio-temporal behavior due to multilateral mode operation, emitting filamented beams with low spatial coherence. Using weak external optical feedback we demonstrate that some degree of lateral mode selection and pattern stabilization of these lasers can be obtained under appropriate feedback conditions.

(September 4, 1996)

I. INTRODUCTION

Broad area lasers are characterized by laterally wide gain regions which are intended to raise the optical output power by increasing the active cavity volume and lowering the photon density at the output facet [1]- [5]. Although broad-area lasers may operate in the fundamental lateral mode for pump levels close enough to threshold, the spatial coherence and the spectral purity of the output beam are severely degraded as the pump level is increased [3]. In fact, beam filamentation in broad-area lasers has been observed for moderate pump levels. The reason is that in broad-area lasers not only the field dynamics but also the lateral modes themselves (modal profiles and modal frequencies) are determined by the interplay between the lateral gain and refraction index profiles associated with the population inversion distribution. While the population inversion profile tries to confine the field distribution under the pump region because of gain-guiding, the associated distribution of refractive index causes either guiding or anti-guiding, depending on the device, thus reinforcing or opposing the gain-guiding mechanism. The combined effect of the gain and the refractive index makes these devices highly sensitive to destabilizing mechanisms related to changes in the population inversion profile and can thus cause interesting spatio-temporal dynamics.

Experimental measurements [1] in solid-state lasers have displayed the formation of a single filament or periodic arrays of filaments when the laser beam is allowed to self-focus in a nonlinear medium, which was explained in terms of the destabilization of higher order modes due to index and gain variations with the intensity [2]. Laser emission in a stable single filament [3], in a periodic array of filaments [4], and erratic filamentation has been observed in broad-area semiconductor lasers. In the last case, the laser emission consists of one or several filaments moving erratically along the junction plane of the semiconductor laser (lateral direction) on nanosecond time scales [6], and a degraded output beam persists upon time-averaging. Beam filamentation has also been studied from a numerical point of view. Stable multi-filament formation in a unidirectional ring laser has been numerically observed and analyzed, in which case filamentation results as a consequence of the frequency locking of several lateral cavity modes [7]. Also, numerical studies of broad-area semiconductor lasers [6,8,9] show that beam filamentation is due to the onset of higher order lateral modes, that arise from the competition between spatial hole burning, the carrier-induced index change and optical diffraction.

Active dynamical systems (such as lasers) can often be stabilized by introducing a feedback circuit. When the feedback, which can be optical and/or electrical, involves substantial time-delay, one must generally expect the possibility of instabilities associated with chaotic pulsations in the system [10]. Semiconductor lasers are extremely sensitive to optical feedback due to the combination of low facet reflectivities and high gain [11]. Indeed, it was found that semiconductor lasers are already brought into a state of coherence collapse for feedback power levels as low as -40 dB from distant reflectors (> 10 cm) [12]. In this state, the laser field shows a spectral broadening up to $\sim$ 25 GHz, in sharp contrast to its original linewidth of typically 100 MHz. The wealth of nonlinear dynamics associated with this state has attracted a lot of attention [13]– [15]. On the other hand, employing carefully controlled external optical feedback, from not too distant reflectors, can result in substantial stabilization and ensure single longitudinal mode operation with a linewidth reduction up to a factor $\sim$ 1000 [16]– [18].

External optical feedback is characterized by the length of the external cavity, i.e., the cavity formed by the exposed laser facet and the external reflector, and the optical power fed back into the laser cavity. The behavior of the compound cavity system, consisting of the laser cavity and the external cavity, is the result of the nonlinear interaction between the longitudinal mode(s) of the laser on the one hand and the external cavity resonance frequencies on the other hand. By small changes in the external cavity length (on the order of an optical wavelength), the external cavity resonances can be tuned with respect to the laser mode(s) [19]. Thus, external optical feedback can reduce the multimode character of a laser and allow tuning of the resulting single-mode [20].

A numerical study of the spatio-temporal dynamics of both a single narrow stripe and a twin-stripe index-guided semiconductor lasers has shown that external optical feedback can modify the arousal of spatio-temporal instabilities in these lasers [21]. In this paper we investigate whether optical feedback from an external cavity can prevent beam filamentation in broad-area lasers, stabilizing operation in the fundamental, single-lobe lateral mode and providing spatially-coherent, diffraction-limited, high-power laser sources. The influence of the population-inversion induced index change is analyzed, depending on whether it opposes (induced-index anti-guiding) or reinforces (induced-index guiding) the confinement of the field within the pump region.

The outline of the paper is as follows. In Section II we present the model used for the dynamical description of the single-longitudinal-mode, broad-area laser. The model is based on the semiclassical description of a two-level medium, and it incorporates external optical feedback in the Lang-Kobayashi approximation. The Bloch equation for the nonlinear material polarization is retained in the model because it provides a nonlinear susceptibility whose real part associates different gain to the lateral modes, while the imaginary part accounts for the population-inversion induced index change. In Section III we describe the characteristic spatio-temporal dynamics of broad-area lasers obtained by numerical integration of the model equations. In absence of optical feedback we show how laser emission properties are degraded as the pump level applied to the device is raised. For both induced-index guiding and anti-guiding, the spatio-temporal dynamics are qualitatively similar, the main difference being "cleaner" spectra for the guiding case because of the increased mode confinement. After this, the effects of optical feedback are studied. The results show that a certain degree of lateral mode selection can be achieved under appropriate feedback conditions for both induced-index guiding and anti-guiding. Most important is the fact that the current range where fundamental mode emission occurs can be appreciately enlarged only for the guiding case. However, spatio-temporal instabilities can also be induced by slighty changing the feedback conditions resulting in states of low spatio-temporal coherence. Some concluding remarks are presented in Section IV.

II. LASER MODEL

The lasers we consider are single-longitudinal mode, broad-area lasers whose lateral field distribution is determined only by the population inversion profile. We consider that one of the transverse dimensions is narrow enough to support only the fundamental transverse mode, but the laser may oscillate in one or several modes along the other (lateral) dimension.

We model the laser medium as a two-level system, which leads to the semiclassical Maxwell-Bloch equations including optical field diffraction [7,8], population inversion diffusion [22] and the pump profile [9,23]. We write the equations as follows:

$$\begin{aligned}\partial_t E &= -\frac{1-i\theta}{2\epsilon}E + i\ \Delta\ \partial_x^2 E + \frac{P}{2} \\ &\quad + \kappa \exp(i\omega\tau) E(x, t-\tau)\ , \qquad (1)\\ \partial_t P &= -\epsilon\sigma(1+i\theta)P + \sigma(1+\theta^2)D\ E \\ &\quad + \sqrt{\eta_1 + \eta_2 D}\ \chi(x;t)\ , \qquad (2)\\ \partial_t D &= \epsilon(J(x) - D) + \delta\ \partial_x^2 D - \frac{1}{2}[EP^* + E^*P]\ , \qquad (3)\end{aligned}$$

where $E(x,t)$, $P(x,t)$ and $D(x,t)$ describe the slowly varying lateral distributions of the optical field, the material polarization and the population inversion respectively. Δ accounts for optical diffraction, δ describes the population inversion diffusion, $\epsilon = (\gamma_{\|}/\gamma)^{1/2}$ is a measure for the decay rate ratio between optical field γ and inversion $\gamma_{\|}$, and $\sigma = \gamma_{\perp}/\gamma_{\|}$ is the decay rate ratio between the polarization $\gamma_{\perp}$ and the inversion. Spontaneous emission is modeled by means of a complex white noise source ($\chi(x;t)$) whose amplitude is taken as $\eta_1 + \eta_2 D$, corresponding to the linearization around threshold of the spontaneous emission power [24].

The parameter values used in the simulations, ϵ =0.0215 and $\sigma = 3\ 10^4$, are typical for a class B laser where the population inversion variable is the slowest one. The diffraction coefficient Δ =104 corresponds to a wavelength of $\lambda = 0.820\ \mu$m, while the diffusion coefficient $\delta = 0.2$ has an associated diffusion length of $L_D = 3.65\ \lambda$. $J(x)$ is the scaled lateral pump distribution, which we consider to be a supergaussian symmetric distribution centered in the integration region (x=0). The total pump level (I) is obtained by integration of $J(x)$ over the lateral dimension (x) and it is usually expressed in terms of the threshold pump level (I_{th}).

The polarization P acts as a source for the electromagnetic field, providing both gain and changes in the background refraction index of the system. An important parameter is $\theta \equiv (\omega_{mat} - \omega)/\gamma_{\perp}$, the detuning of the carrier frequency, ω, from the material dipole resonance frequency, ω_{mat}. The effect of the detuning in Eqs. (1)-(3) is twofold. On one hand it determines the change in refraction index induced by population inversion: for positive (negative) θ, an increase in population inversion is accompanied by a decrease (increase) in the index of refraction, thus yielding induced-index anti-guiding (guiding) and opposing (reinforcing) the gain-guiding mechanism for the field. On the other hand, the sign of θ strongly affects the stability of the fundamental lateral mode, as analyzed by Jakobsen *et al.* [22] in the case of an infinite pump region. It was shown that for negative detuning ($\theta < 0$) the fundamental ($k = 0$) lateral mode is the first one to reach threshold, while for positive detuning ($\theta > 0$) the mode which first becomes unstable is a lateral mode with $k \neq 0$. The reason is that higher lateral modes have higher frequency, since the diffraction coefficient Δ is positive by definition; so, for negative detuning the gain of the fundamental mode is the highest, while for positive detuning some lateral mode with $k \neq 0$ is the closest to the gain peak [25]. We should remark that this analysis corresponds to a laser with an infinite pump region, so the k form a continuous set. In a real system, the finite dimensions of the pump region limit the maximum lasing k and provide a frequency separation between the transverse modes in such a way that the wider the pump region, the smaller the frequency separation between transverse modes. In this situation, the possibility of laser emission in a higher order mode will depend on the the pump region widths and the detuning values chosen. In this paper, the detuning is always smaller than the frequency separation between lateral modes, so the fundamental mode is always selected at threshold, and it will be shown that both situations, induced-index guiding and anti-guiding, are almost equivalent in terms of the number of excited lateral modes, the only difference being the confinement of these modes. We note that laser emission in the fundamental mode or in a higher order mode as a function of the detuning has been experimentally observed in VCSEL's [26].

Our model adequately describes homogeneously broadened two-level lasers (such as solid-state or dye lasers). It does not correctly describe semiconductor lasers, since for those systems the gain is asymmetric, and even when they operate close to the gain peak, they exhibit a very strong anti-guiding effect. Typically, the anti-guiding factor for semiconductor lasers is $1 < \alpha < 10$, where α is also known as the linewidth enhancement factor [27]. This can not be modeled by simply putting the detuning θ equal to α, because when doing so, the laser emission (forced far away from the gain peak) will ultimately operate close to the gain peak, where $\theta \sim 0$. Recent models to describe the semiconductor polarization dynamics macroscopically contain at least one extra parameter in the polarization equation [28,29].

In view of the above, we have limited the values of the detuning $\mid \theta \mid < 0.25$ [30], and consider our model given by Eqs. (1)-(3), as a generic model which provides useful information on general features of broad-area devices.

The last term in Eq. (1) accounts for weak optical feedback from an external mirror positioned at a distance $L_{ext} = c\tau/2$, where c is the speed of light in vacuo and τ is the round-trip time from the laser to the external mirror and back. Only one round-trip time is taken into account, which is a good approximation if the feedback is weak enough [31]. We neglect all diffraction of the light in the external cavity. This is justified if L_{ext} is very small, or when a lens is put in the external cavity that images the output beam back into the laser. We have chosen this simple configuration because in more practical systems (e. g. a collimating system formed by a spherical and a cylindrical lens), the field reinjected at one point is a complicated functional of the output field profile, which would increase the complexity of our model even further. The parameter κ is the feedback-rate, whose square is a measure for the feedback power ratio. The factor $\omega\tau$ is called the feedback phase, and is the result of the slowly-varying amplitude description. Small variations in L_{ext} (and therefore in τ), corresponding to a quarter of an optical wavelength cause the feedback phase to change π, which implies a change from constructive to destructive interference. Indeed, control over the feedback phase is a necessary condition to observe many of the feedback effects [32]. For practical purposes, i.e, $L_{ext} > 1000\lambda$, the feedback phase $\omega\tau \bmod(2\pi)$ can be regarded as an independent feedback parameter [14]. Feedback is therefore described by κ, τ, and $\varphi_{fb} = \omega\tau \mathrm{mod}(2\pi)$.

Although the feedback power level is proportional to κ^2, the effective feedback strength for single-mode lasers is often expressed by the dimensionless number [31]:

$$C = \kappa \; \tau \; \sqrt{1+\theta^2} \; . \tag{4}$$

In the limit of class-B lasers, the magnitude of C is a good estimate for the number of active compound-cavity modes, i.e., longitudinal modes that are the result of the nonlinear interaction between the single longitudinal laser mode and the external cavity resonances, which have a frequency spacing of $1/\tau$ [31]. In this paper we will always consider $C < 1$, so that only one longitudinal mode is active.

III. NUMERICAL RESULTS

In order to analyze to which extent optical feedback may be used for lateral mode control and stabilization in broad-area lasers, we have numerically solved Eqs. (1)-(3) using the same procedure as in [9,23].

A. Broad Area Spatio-Temporal Dynamics

1. Positive Detuning

In Fig. 1 we show the Time-Resolved Near-Field (TRNF) profile $|E(x,t)|^2$, and in Fig. 2 the Spectrally-Resolved Near-Field (SRNF) of a solitary (no feedback) broad-area laser with a pump region of width 10 L_D, operating with positive detuning $\theta = 0.25$ (population inversion induced index anti-guiding) for different pump levels.

The laser operates in the fundamental lateral mode up to the pump value $I \sim 1.15\ I_{th}$. Up to this pump level, the optical power (Fig. 1a) shows the typical relaxation oscillation behavior after the turn-on. The frequency of the oscillation is proportional to the square root of the pump, as expected. After this transient the system reaches a steady state pattern profile which consists of a stationary bell-shaped lobe with the maximum intensity in the center of the spatial population inversion lateral distribution, as shown by the SNRF (Fig. 2a).

For pump levels between 1.15 I_{th} and 1.6 I_{th} the first part of the transient behavior is similar, but before the relaxation oscillations have decayed, the single lobe is destabilized and starts bouncing across the gain region almost periodically (see Fig. 1b). This kind of behavior can be explained in terms of spatial hole burning and the competition between gain-guiding and the induced-index anti-guiding effect (the refraction index is higher in the regions of lower population inversion). Initially, the laser beam profile is single-lobed and centered on the pump profile. The stronger stimulated recombination that occurs at the center of the pump region, burns a spatial hole in the center of the population inversion which cannot be washed-out by diffusion immediately [33]. Since the refractive index is larger at the center of the pump region, the beam is locally self-focused. As the pump level is increased, the hole at the center of the population inversion distribution becomes more pronounced (thus locally enhancing beam self-focusing) and the population inversion in the outer regions increases. The population inversion gain-guiding effect and the beam self-focusing effect compete to confine the optical field and, when the pump becomes large enough, the gain-guiding effect dominates, forcing the intensity peak to move to one of the sides of the population inversion distribution. The stronger stimulated recombination now occurs on this side, decreasing the population inversion in this region, and forcing the movement of the filament to the other side, where the process repeats again. The SRNF corresponding to this situation (Fig 2b) shows that the fundamental and first higher-order lateral modes are simultaneously excited, with the two-lobe mode carrying almost the same power as the fundamental lateral mode. The spatio-temporal dynamics of the intensity is intimately related to the coexistence of both lateral modes, because the bouncing period for the lobe across the gain region corresponds exactly to the beat note of the two excited modes.

As the pump level is further increased, $I \geq 1.6\ I_{th}$, the light beam presents a higher number of lobes. Fig. 1c shows the case $I = 2.0\ I_{th}$. The intensity profile consists of one or several filaments which appear, move, and vanish within the stripe. Diagonal propagation of the filaments, migrating from one side of the stripe to the opposite one, is observed as in semiconductor broad-area lasers [6]. The SRNF in Fig. 2c shows that the number of lateral modes oscillating simultaneously has increased to three, but it is worth noting that now the modes are no longer sharply defined as in the previous cases, but instead are substantially broadened, with noticeable fractions of power being smeared-out around the different spectral peaks. The temporal and spatial coherence of the system is strongly reduced, yielding both a broad power spectrum of the laser and an erratic far-field.

2. Negative Detuning

Similar spatio-temporal dynamics are observed when the laser is operated on the negative detuning side, although in this case one has population inversion induced index guiding (the higher the gain the higher the refraction index). Fig. 3 shows the SRNF for $\theta = -0.25$ and different pump levels. It should be noted that now the modal peaks are sharper than those in Fig. 2. The reason is that for $\theta < 0$ there is a real waveguiding mechanism associated to pump, which contributes to stabilize the lateral modes. Oppositely, for $\theta > 0$, there is not a real waveguiding effect, so all modes would be leaky if gain was disregarded.

B. Optical Feedback

In this section we study the effects of applying weak external optical feedback to the broad-area laser. In all the simulations, we first let the system achieve its steady-state without optical feedback ($\kappa = 0$) as was done in the previous section (Fig. 1). After this, the feedback is instantaneously switched-on. We use an external cavity length of $L_{ext} = 2600\ \lambda$, which corresponds to a delay-time of $\sim$ 14.2 ps ($\tau = 0.222$). Tuning of the cavity length over half an optical wavelength, i.e., $\Delta L_{ext} = 2 \times 10^{-4}$ will hardly affect the delay-time, but will cause a change in the feedback phase of 2π. Experimentally, such length-tuning can be achieved through the use of a PZT. This short cavity provides an external cavity resonance spacing of $\sim 210\gamma_{\|}$ which is much larger than the spectral width of the free-running laser. Thus, by varying the feedback phase one of the external cavity resonances can be tuned over the entire free-running laser spectrum, and by choosing $C \sim 0.45\ < 1$, single-longitudinal mode operation of the compound cavity (laser cavity + external cavity) is ensured. The position of the external cavity resonances as a function of the feedback phase is given in Table I.

1. Positive Detuning

We first consider the case I=1.15 I_{th} with $\theta = 0.25$. In absence of feedback (Fig. 4a), the laser operates in the fundamental lateral mode. Taking a feedback-rate of $\kappa = 2$, the actual value of φ_{fb} is very important for the outcome: Fig. 4b and 4c show the SRNF of the laser with optical feedback for two different feedback phases ($\varphi_{fb} = \pi/2$ and $\varphi_{fb} = \pi$) corresponding to different behavior regimes. When the feedback phase is in the range $\pi < \phi_{fb} < \frac{3\pi}{2}$, both the fundamental and the first order lateral mode are simultaneously excited, while for all other values the system remains single-lateral mode, although pulling of its frequency occurs. This behavior can be explained by considering the relative positions of the laser mode and the external cavity resonances (see table I). For $\phi_{fb} \leq \pi$, the frequency of the external cavity mode ν_m is close to that of the fundamental lateral mode of the free-running laser, while those of modes $\nu_{m\pm1}$ correspond to values much higher and lower, respectively, than the spectral width of the free-running laser. As a consequence, the dynamics of the system is dominated by the external cavity mode ν_m, whose main effect is to pull the frequency of the fundamental lateral mode as the feedback phase is varied. This effect is the same occurring in single-mode lasers under weak optical feedback, where the emission frequency of the system shifts as the feedback phase is varied [34]. However, in the range where $\pi < \phi_{fb} < \frac{3\pi}{2}$, the mode ν_{m+1} becomes closer to the free-running laser spectrum than ν_m, and will influence the dynamics of the system. For this range of feedback phases, the external mode ν_{m+1} is closer to the first higher order mode of the free-running laser, which results in the simultaneous excitation of both the fundamental and the first higher order mode. For $\phi_{fb} > \frac{3\pi}{2}$ we recover single-lateral mode emission since the external cavity mode ν_{m+1} is now closer to the fundamental one.

As we have previously seen (Figs. 2 and 3), for pump levels larger than $1.15 I_{th}$ and in absence of feedback, the broad-area laser enters in the multi-lateral mode regime, so simultaneously two or more lateral modes are present. In this case, external optical feedback could be applied in order to try to suppress a lateral mode from the output pattern. This is the situation for a pump level 1.2 I_{th} in the anti-guiding case (θ =0.25). We have applied optical feedback of different strenghts ($\kappa \leq 2$) to the system in order to force emission in the fundamental mode, but we could never obtain stable emission in the fundamental mode. However, in a small range of feedback phases around $\phi_{fb} = \frac{\pi}{2}$, the system maintains this highly coherent state during a long time, but it finally returns to the multi-lateral mode situation. In order to try to reach indefinite fundamental mode operation we reduced the pump level and increased the feedback strength (within the range $C < 1$), but we only achieved an increase of the life-time of the fundamental mode state.

2. Negative Detuning

A completely different behavior is obtained for the population inversion induced index-guiding case ($\theta < 0$). Fundamental mode operation assisted by optical feedback is found to be stable up to pump values $I \leq 1.38$ I_{th}, while the range of feedback phases for which the fundamental mode is stabilized decreases as the injection current increases. Fig. 5a and Fig. 3b show the TRNF and the SRNF respectively, for a pump value 1.3 I_{th} and θ=-0.25 when no optical feedback is applied. The laser emits simultaneously with two lateral modes. However, after applying weak optical feedback ($\kappa = 2$) at $t * \gamma_{\|}$=5, fundamental lateral mode operation is achieved for feedback phases in the range $\frac{3\pi}{8} < \phi_{fb} < \frac{5\pi}{8}$. Fig. 5b and Fig. 6a show how the fundamental mode is stabilized after some relaxation oscillations for $\phi_{fb} = \frac{\pi}{2}$. As a difference to what occurs for the positive detuning case, pattern stabilization occurs here because the population inversion distribution not only provides the gain necessary for laser action, but it also provides good optical field confinement through the associated refraction index change.

Other dynamical situations are observed when the feedback phase is changed to values outside the single lateral mode emission range. Simultaneous operation in the first, second and third lateral modes is obtained for $\frac{3\pi}{4} < \phi_{fb} < \frac{5\pi}{4}$ (Fig. 6b), while the laser recovers operation in the fundamental and first order lateral modes for the other feedback phases (Fig. 6c). Again, the dynamics can be explained through the nonlinear interaction of the external cavity resonances with the free-running laser modes, as was done for $I = 1.15$ I_{th} and $\theta = 0.25$.

For pump levels larger than 1.38 I_{th}, fundamental mode operation is never achieved for the feedback strength considered, as it already occurs for positive detunings. The reason is that at this pump levels, the modal gain (overlapping of the population inversion distribution and the mode profile) for the fundamental lateral mode is very small because of the strong spatial hole burning in the center of the population inversion distribution. Lasing of the first higher order mode (two-lobes mode) is favored because the population inversion distribution coincides at this pump levels with the mode profile, so the modal gain for the two-lobe mode is very large. In addition, the optical feedback strength is small enough to compete with the gain mechanism, and pattern stabilization of the fundamental mode is not achieved.

As the pump level is increased, the number of lateral modes simultaneously oscillating also increases. However, a certain degree of lateral mode control can still be achieved. Fig. 7 shows the TRNF and the SRNF for weak optical feedback ($C = 0.45$) and different feedback phase values, at a pump level twice the lasing threshold. In absence of optical feedback (Fig. 3c) the first three lateral modes are simultaneously excited at this pump level. The application of external optical feedback and an appropriate selection of the feedback phase can reduce the number of oscillating modes to two (Fig. 7a), increase this number to four (Fig. 7b), or leave it unchanged (Fig. 7d). States of strong filamentation are also observed (Fig. 7c), where the spectral power is quasi-continuously distributed over a wide range of frequencies, indicating a very short coherence time.

For pump levels larger than 1.38 I_{th} and positive detunings, dynamic behaviors similar to those obtained for negative detuning have been observed within the same feedback-phase ranges, the main difference being in the lateral mode confinement which affects the SRNF.

IV. CONCLUSIONS

In this paper we have studied the spatio-temporal dynamics of broad-area Class-B lasers through a generic model based on the two-level model approach. The results found in Subsec. III A for both positive and negative detuning, show a striking resemblance to the experimental results obtained with a broad-area semiconductor laser [3,6]. However, the detuning values used in the simulations are very small as compared to the typical values of the α–paramenter in semiconductor lasers. This results may indicate that the spatio-temporal dynamics of semiconductor lasers are strongly dominated by the spatial effects as population inversion diffusion and optical field diffraction, while the index anti-guiding effect introduced by the α–paramenter will slighty affect the dynamics. Another possibility is that the induced index anti-guiding associated to the α factor is compensated by thermal lensing effects in the pump region.

We have studied the stabilization of fundamental-mode emission by weak optical feedback, which modifies the spatio-temporal dynamics of these devices. Optical feedback is described in the Lang-Kobayashi approximation, and several situations have been studied depending on the detuning parameter, the pump level and the feedback phase values. The results show that a certain degree of lateral mode control can be achieved in broad-area lasers by applying external optical feedback with appropriately chosen feedback phases. Lateral mode enhancement or suppression are observed in both positive and negative detuning device operations, always for a fix value of the optical feedback strength (fix external mirror reflectivity), and variations of the feedback phase between 0 and 2π (which correspond to variations of the external cavity within half a wavelength). However, stabilization of the emission pattern, where the laser is forced to emit in the fundamental lateral mode by optical feedback at pump values for which the broad-area laser natural emission is multi-lateral, is only found when the broad-area laser is operated with negative detuning.

V. ACKNOWLEDGEMENTS

This work has been partially supported by CICYT Projects No. TIC95/0563, and PB94-1167 (Spain), and CHRX-CT-94-0594.

[1] A. J. Campillo, S. L. Shapiro, and B. R. Suydam, *Appl. Phys. Lett.*, **23**, 628, (1973);
A. J. Campillo, S. L. Shapiro, and B. R. Suydam, *Appl. Phys. Lett.*, **24**, 178, (1974).

[2] Bespalov, V.I., and Talanov, B.I., *Sov. JETP Lett*, **3**, 307, (1966).

[3] C. J. Chang-Hasnain, E. Kapon, and R. Bhat, *Appl. Phys. Lett.*, **54**, 205, (1989).

[4] R. J. Lang, D. Mehuys, A. Hasrdy, K. M. Dzurko, and D. F. Welch, *Appl. Phys. Lett.*, **62**, 1209, (1993).

[5] M. Tamburrini, L. Goldberg, and D. Mehuys, *Appl. Phys. Lett.*, **60**, 1292, (1992).

[6] I. Fischer, O. Hess, and W. Elsässer, *Nonlinear Dynamics in Optical Systems*, June 1995, Rochester, New York, USA.

[7] L. A. Lugiato, C. Oldano, and L. M. Narducci, *J. Opt. Soc. Am. B*, **5**, 879, (1988).

[8] O. Hess, S. W. Koch, and J. V. Moloney, *IEEE J. Quantum Electron.*, **31**, 35, (1995).

[9] J. Martin-Regalado, S. Balle, and N. B. Abraham, *IEE Proc. Optoelectronics*, vol. **143**, 17 (1996).

[10] A. B. Pippard, "Response and Stability: An Introduction to the Physical Theory," (Cambridge: Cambridge University Press), 1985.

[11] R. Lang and K. Kobayashi, *IEEE J. Quantum Electron.*, **QE-16**, 347, (1980).

[12] D. Lenstra, H. Verbeek, and A. J. den Boef, *IEEE J. Quantum Electron.*, **QE-21**, 674, (1985).

[13] J. Mørk, J. Mark, and B. Tromborg, *Phys. Rev. Lett.*, **65**, 1999 (1990).

[14] G. H. M. van Tartwijk, A. M. Levine, and D. Lenstra, *IEEE J. Sel. Top. Quantum Electron.*, **1**, 466 (1995).

[15] I. Fischer, G. H. M. van Tartwijk, A. M. Levine, W. E. Elsässer, E. O. Göbel, and D. Lenstra, *Phys. Rev. Lett.*, **76**, 200 (1996).

[16] L. Goldberg, H. F. Taylor, A. Dandridge, J. F. Weller, and R. O. Milles *IEEE J. Quantum Electron.*, **18**, 555, (1982); N. Chinone, K. Aiki, and R. Ito, *Appl. Phys. Lett.*, **32**, 990, (1978).

[17] E. Patzak, H. Olesen, A. Sugimura, and T. Mukai, *Electron. Lett.*, **19**, 938 (1983).

[18] G. P. Agrawal, *IEEE J. Quantum Electron.*, **QE-20**, 468 (1984).

[19] A. M. Levine, G. H. M. van Tartwijk, D. Lenstra, and T. Erneux, *Phys. Rev. A*, **52**, 3436 (1995).

[20] M. Homar , J. V. Moloney and M. San Miguel, *IEEE J. Quantum Electron.*, **32**, 553, (1996).

[21] M. Münkel, F. Kaiser, and O. Hess, Accepted.

[22] P.K. Jakobsen, J. V. Moloney, A. C. Newell, and R. Indik, *Phys. Rev. A.*, **5**, 8129, (1992).

[23] J. Martin-Regalado , S. Balle, and N. B. Abraham, *IEEE J. Quantum Electron.*, **32**, 257, (1996).

[24] S. Balle, M. San Miguel, N. B. Abraham, J. R. Tredicce, R. Alvarez, E. J. D'Angelo, A. Gambhir, K. Scott Thornburg, and R. Roy, *Phys. Rev. Lett.*, **72**, 3510 (1995).

[25] A. C. Newell, in "Lecture Notes for European Science Foundation Study Center", Nonlinear Optics and Guided Waves, University of Edinburg, August 1994.

[26] T. J. Rogers, D. L. Huffaker, H. Deng, Q. Dengm, and D. G. Deppe, *IEEE Phot. Tech. Lett.*, **7**, 238, (1995).

[27] C. H. Henry, IEEE J. Quantum Electron., **QE-18**, 259 (1982).

[28] S. Balle, *Optics Comm.*, vol. **119**, 227 (1995).

[29] J. Yao, G. P. Agrawal, P. Gallion, and C. M. Bowden, Optics Comm., **119**, 246 (1995).

[30] C. Etrich, P. Mandel, N. B. Abraham, and H. Zeghlache *IEEE J. Quantum Electron.,* **28**, 811 (1992).

[31] G. H. M. van Tartwijk and D. Lenstra, *Quantum Semiclass. Opt.*, **7**, 87 (1995).

[32] J. Mørk, M. Semkow, and B. Tromborg, *Electr. Lett.*, vol. **26**, 609 (1990).

[33] B. W. Hakki, *J. Appl. Phys.*, **46**, 292, (1975).

[34] J. O. Binder, and G. D. Cormack, *IEEE J. Quantum Electron.*, **25**, 2255, (1989).

External Cavity Mode Frequency as a function of the Feedback Phase

ϕ_{fb}	$\nu_{m-1}/\gamma_{\|\|}$	$\nu_m/\gamma_{\|\|}$	$\nu_{m+1}/\gamma_{\|\|}$
0	-210.000	0.000	210.000
$\frac{\pi}{4}$	-236.250	-26.250	183.750
$\frac{\pi}{2}$	-262.500	-52.500	157.500
$\frac{3\pi}{4}$	-288.750	-78.750	131.250
π	-315.000	-105.000	105.000
$\frac{5\pi}{4}$	-341.250	-131.250	78.750
$\frac{3\pi}{2}$	-367.500	-157.500	52.500
$\frac{7\pi}{4}$	-393.750	-183.750	26.250
2π	-420.000	-210.000	0.000

TABLE I. Position of the external cavity resonances as a function of the feedback phase

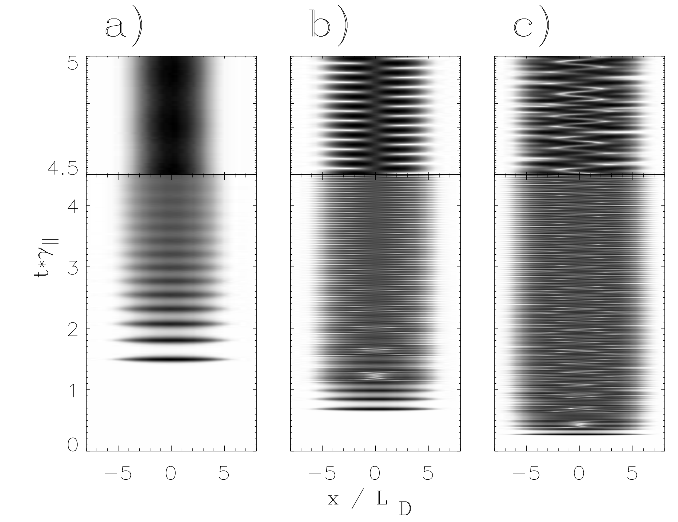

FIG. 1. TRNF of an index anti-guided broad-area laser. The light power emitted at each point of the laser facet is plotted versus the normalized time using a 256-level grey-scale, with black corresponding to the maximum value and white to the minimum. The plots correspond to κ=0.0, θ=0.25, and different current levels: a) 1.1 I_{th}, b) 1.3 I_{th}, c) 2.0 I_{th}. Other parameters are given in the text. To improve the resolution of the pictures we have expanded the time axis when the laser reaches the steady-state

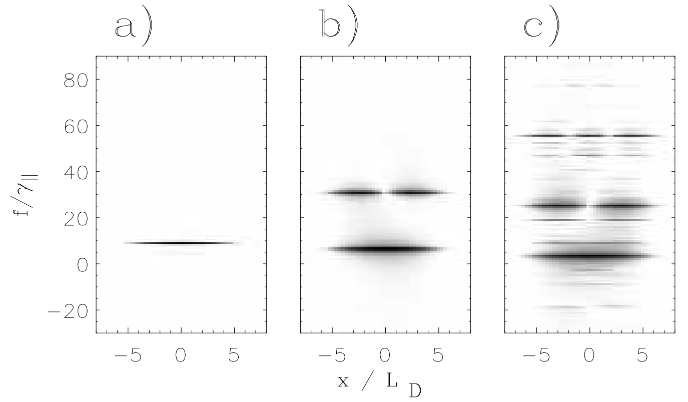

FIG. 2. SRNF of an index anti-guided broad-area laser. The field power spectrum of the broad-laser is resolved for each point of the laser facer and plotted versus frequency using a 256-level grey-scale. Same parameter values as in Fig. 1

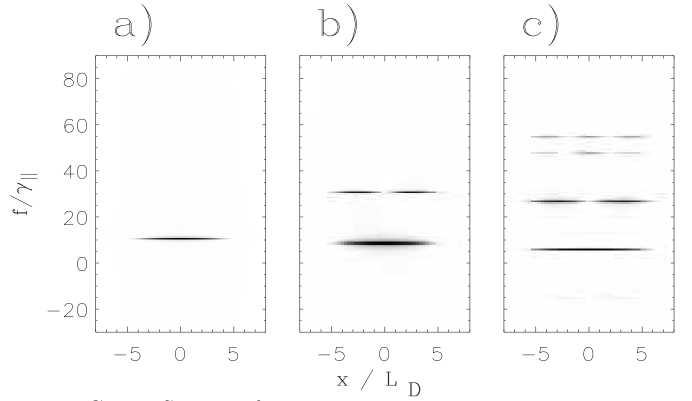

FIG. 3. SRNF of a index-guided broad-area laser with κ=0.0, θ=-0.25, and different current levels: a) 1.1 I_{th}, b) 1.3 I_{th}, c) 2.0 I_{th}.

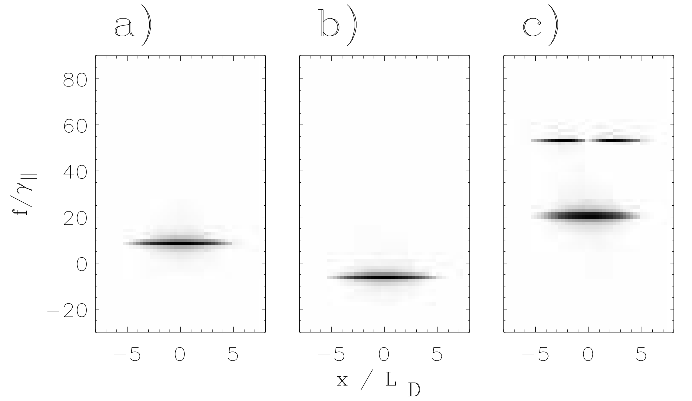

FIG. 4. Optical feedback effects for the single-lateral mode situation with 1.15 I_{th} and θ=0.25 (index anti-guiding). a) $\kappa = 0$, no feedback; b) $\kappa = 2$, $\phi_{fb} = \frac{\pi}{2}$; and c) $\kappa = 2$, $\phi_{fb} = \pi$.

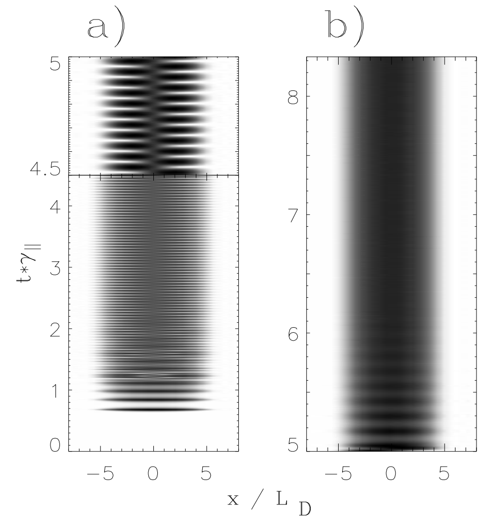

FIG. 5. Stabilization of the fundamental lateral mode through optical feedback for a index-guided broad-area laser. a) $\kappa = 0$, without optical feedback the laser has multi-lateral mode emission; b) $\kappa = 2$, $\phi_{fb} = \frac{\pi}{2}$, with optical feedback the laser can reach monomode stable operation. The pump level is 1.30 I_{th} and θ=-0.25.

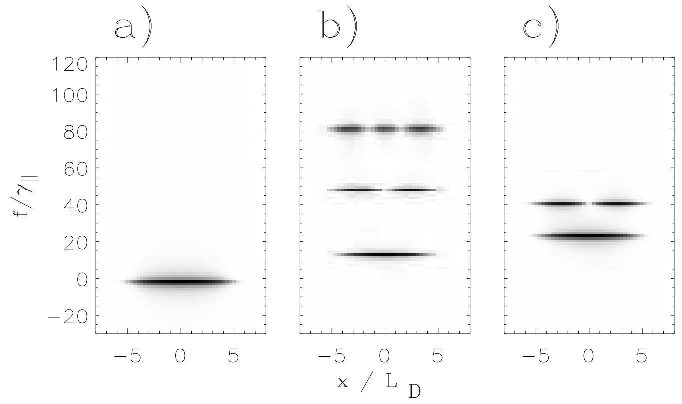

FIG. 6. SRNF of a broad-area laser at I=1.30 I_{th} and $\theta = -0.25$. The SRNF shows different kind of dynamics as the feedback phase is varied: a) $\phi_{fb} = \frac{\pi}{2}$; b) $\phi_{fb} = \pi$; and c) $\phi_{fb} = \frac{3\pi}{2}$.

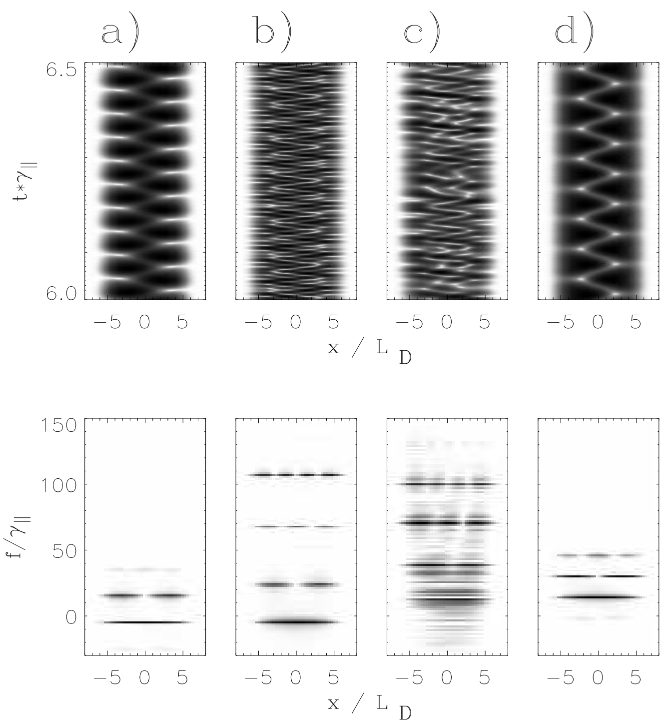

FIG. 7. TRNF and SRNF of a broad-area laser at I=2.0 I_{th} and $\theta = -0.25$ under the effects of weak optical feedback and appropriate selection of the feedback phase: a) $\frac{\pi}{2}$, b) $\frac{3\pi}{4}$, c)π , and d) $\frac{7\pi}{4}$.